Naunyn-Schmiedeberg's Archives of Pharmacology
https://doi.org/10.1007/s00210-024-03320-3

RESEARCH

Molecular mechanism of geniposide against ANIT-induced intrahepatic cholestasis by integrative analysis of transcriptomics and metabolomics

Junyi Zhang[1] · Yunting Chen[1] · Guangming Luo[1] · Yangjing Luo[1]

Received: 19 April 2024 / Accepted: 18 July 2024

Abstract

Geniposide (GE), a bioactive compound extracted from the fruit of *Gardenia jasminoides* Ellis, has attracted significant attention for its hepatoprotective therapeutic applications. Although GE displays a protective effect on treating intrahepatic cholestasis (IC), the underlying mechanism remains elusive. In this study, we aimed to elucidate the pharmacological mechanisms of GE in treating IC by an integrated analysis of transcriptomics and metabolomics. Firstly, we evaluated the hepatoprotective effect of GE in α-naphthylisothiocyanate (ANIT)-induced IC rats by examining biochemical indices, inflammatory factors, and oxidative stress levels. Secondly, by transcriptomics and serum metabolomics, we identified differentially expressed genes and metabolites, revealing phenotype-related metabolic pathways and gene functions. Lastly, we screened the core targets of GE in the treatment of IC by integrating transcriptomic and metabolomic data and validated these targets using western blotting. The results indicated that GE improved serum indexes and alleviated inflammation reactions and oxidative stress in the liver. The transcriptomics analysis revealed 739 differentially expressed genes after GE treatment, mainly enriched in retinol metabolism, steroid hormone synthesis, PPAR signal transduction, bile secretion metabolism, and other pathways. The metabolomics analysis identified 98 differential metabolites and 10 metabolic pathways. By constructing a "genes-targets-pathways-compounds" network, we identified two pathways: the bile secretion pathway and the glutathione pathway. Within these pathways, we discovered nine crucial targets that were subsequently validated through western blotting. The results revealed that the GE group significantly increased the expression of ABCG5, NCEH1, OAT3, and GST, compared with the ANIT group. We speculate that GE has a therapeutic effect on IC by modulating the bile secretion pathway and the glutathione pathway and regulating the expression of ABCG5, NCEH1, OAT3, and GST.

Keywords Geniposide · Intrahepatic cholestasis · Transcriptomic · Metabolomic · Bile secretion pathway · Glutathione pathway

Introduction

Intrahepatic cholestasis (IC) is a complex disease characterized by disorders in bile production, secretion, and excretion, ultimately resulting in the accumulation of excessive bile acids in the liver (Pfister et al. 2022). The etiologies of IC are multifaceted, including autoimmune diseases such as primary biliary cholangitis, primary sclerosing cholangitis, and autoimmune cholangitis (Hassan and Hertel 2022), hormonal factors such as pregnancy (Hobson et al. 2022), and environmental influences such as drugs and alcohol (Ivashkin et al. 2018; Vitale, et al. 2023). Currently, IC presents significant challenges in treatment. U.S. Food and Drug Administration (FDA) has approved ursodeoxycholic acid (UDCA) and obeticholic acid (OCA) as the primary medications for the treatment of IC liver disease (Levy et al. 2023). However, approximately 40% of IC patients are insensitive to ursodeoxycholic acid treatment, and over 90% of patients experience adverse reactions after treatment with OCA (Corpechot et al. 2011; Hirschfield et al. 2015; van Hooff et al. 2024). Therefore, there is an urgent necessity

✉ Guangming Luo
19830076@jxutcm.edu.cn; Jzlgm88@163.com

✉ Yangjing Luo
lyj_20080819@126.com

[1] College of Pharmacy, Jiangxi University of Chinese Medicine, Nanchang, Jiangxi, China

Published online: 25 July 2024

to investigate innovative treatment approaches that can effectively address the challenges presented by cholestatic liver diseases. In recent years, Chinese herbal medicines have demonstrated promising effects in the prevention and treatment of cholestasis (Kowdley et al. 2018; Fang et al. 2022). By targeting multiple pathways and mechanisms, these herbal medicines may provide a more comprehensive and individualized treatment approach for IC patients.

Geniposide (GE), a natural compound found in the fruits of *Gardenia jasminoides* Ellis, has garnered significant interest among researchers due to its diverse pharmacological properties (Gao and Feng 2022). In recent years, modern pharmacology research has revealed wide pharmacological activities of GE, including anti-diabetic, anti-inflammatory, analgesic, anti-tumor, anti-oxidative, neuroprotective, hepatoprotective, and cholagogic effects (Zhou et al. 2019; Hu et al. 2020; Yuan et al. 2020; Liu et al. 2022a, b). Although GE has been shown to alleviate the symptoms associated with IC, the underlying mechanism remains enigmatic (Tan et al. 2016a, b). The integration of multi-omics data offers a reliable approach to gaining a deeper understanding of the hepatoprotective activities of GE.

The advent of high-throughput technologies has led to the generation of vast amounts of omics data, which describe various biological processes such as gene transcription, protein expression, and metabolite profiles. These data provide assistance in understanding the complex pathogenesis of disease (Picard et al. 2021). Transcriptomics, a key component of omics research, facilitates the study of gene expression and regulation. By analyzing transcriptome information, we can gain a deeper understanding of how genes are translated into proteins and how these proteins function within cells (Salmen et al. 2022). It is crucial for identifying biomarkers and gaining insights into disease mechanisms (Saviano et al. 2020). On the other hand, metabolomics mainly uses high-throughput detection and data processing to uncover the changes in the status and function of small molecules and metabolites (Kim 2021). It contributes to the systematic analysis of metabolites in physiological and pathological processes, which has been increasingly used to explain the biological interactions of diseases (Santos et al. 2023). However, the traditional single-omics approach, which focuses solely on a single layer of biological information, such as transcriptomics or metabolomics, has limitations (Misra et al. 2018). Diseases often involve complex molecular pathways that span multiple biological levels, including gene transcription, protein expression, and metabolite metabolism (Menyhárt and Győrffy 2021). To comprehend these complex interactions, a more comprehensive approach is necessary (Yan et al. 2018). Multi-omics studies, which integrate data from multiple omics layers, have emerged as a powerful tool to address this challenge, aiming to provide a more holistic view of biological systems (Lloyd-Price et al. 2019).

In this study, we aimed to explore the pharmacological mechanisms of GE in treating IC through an integrative analysis of transcriptomics and metabolomics. The gene expression, biomarkers, and signaling pathways induced by GE were analyzed and identified. Additionally, we conducted western blotting to validate the key targets. These studies provided novel insights into the development of more effective therapeutic approaches against IC.

Materials and methods

Materials and reagents

Geniposide (C17H24O10, purity > 98%) was purchased from Yuanye Bio-Technology (Shanghai, China). ANIT and bifendate were purchased from Macklin Biochemical Co., Ltd. (Shanghai, China). Antibodies to ABCG5, ABCG8, SULT2A1, OAT3, NCEH1, SLC10A1, KCNN2, GST, NAT8, and GAPDH were obtained from Protein-Tech Group (Chicago, USA). Alanine aminotransferase (ALT), aspartate aminotransferase (AST), alkaline phosphatase (AKP), total bilirubin (TBIL), direct bilirubin (DBIL), total bile acid (TBA), superoxide dismutase (SOD), malondialdehyde (MDA), and glutathione (GSH) kits were obtained from Wepon Pharmaceutical Co., Ltd. (Taizhou, China).

Animals

Sprague–Dawley rats, weighing between 180 and 220 g, were obtained from Hunan SJA Laboratory Animal Co., Ltd. (Hunan, China, Permission No. SCXK(Xiang)2019–0004). Before the experiment, all rats were accommodated in a rearing room maintained at a temperature of 25 ± 2 ℃ and were provided unrestricted access to food and water for at least a week to facilitate adaptation. All animal care and experimental protocols were approved by the Animal Ethics Committee of the Jiangxi University of Chinese Medicine (Ethical approval No.: JZLLSC20220579).

Forty-eight rats were randomly divided into six groups ($n = 8$ per group): control group, ANIT model group, bifendate group (150 mg/kg), GE high-dose group (100 mg/kg), GE medium-dose group (50 mg/kg), and GE low-dose group (25 mg/kg). The GE groups and the bifendate group were given intragastric administration of GE or bifendate once a day for 7 days, respectively. The control group and the ANIT group were given the same volume of saline. On the 5th day, 2 h after administration, the control group was given olive oil, while the other groups were modeled with a 75 mg/kg ANIT olive oil solution.

Sample collection and preparation

After anesthesia with pentobarbital sodium, the rats in each group were sacrificed for the collection of blood samples and liver tissues. The blood samples were centrifuged at 3000 rpm for 15 min at 4 ℃ and subsequently stored at − 80 ℃. Liver tissues were fixed in a 4% paraformaldehyde solution. Other liver tissues were immediately frozen in liquid nitrogen and also stored at − 80 ℃. The centrifuged blood samples and frozen liver tissues were all prepared for further analysis and experimentation.

Histopathology and biochemical analysis

The fixed liver tissue specimens were paraffin-embedded and sectioned. Sections were stained with hematoxylin and eosin (H&E). The levels of ALT, AST, AKP, TBA, TBIL, DBIL, SOD, MDA, GSH, interleukin 6 (IL-6), interleukin 1β (IL-1β), and tumor necrosis factor-α (TNF-α) were measured using ELISA kits according to the manufacturer's recommendations.

RNA-Seq analysis

Rat liver tissues were selected from the control group, the ANIT group, and the GE high-dose group for experiments. Three samples were randomly selected from each group. The total mRNA of liver tissues was extracted using a Trizol assay kit. mRNA purification, reverse transcription, library construction, and sequencing were performed using the Illumina NovaSeq Reagent Kit method. The sequencing results were compared with reference genomes with HISAT2 software. The differential expression of genes (DEGs) between multiple groups was identified and analyzed using DESeq2 software. DEGs were mapped with Gene Ontology (GO) and Kyoto Encyclopedia of Genomes (KEGG) to determine their functional and biological properties. GO functional enrichment and KEGG pathway analyses were performed with Goatools and KOBAS (Jin et al. 2022).

The RNA sequencing data (BioProject accession number PRJNA934684) reported in this paper have been deposited into the Sequence Read Archive (SRA) database.

Metabolomics analysis

Metabolite extraction

The control group, the ANIT group, and the GE high-dose group were selected for metabolomics. The metabolites in the serum samples were extracted by following the established protocol (Song et al. 2023). A total of 100 µL liquid sample was blended with 400 µL solution composed of acetonitrile and methanol in a 1:1 ratio (v:v), containing 0.02 mg/mL of L-2-chlorophenylalanine as an internal standard, to facilitate the extraction of metabolites. The samples were mixed by vortex for 30 s and low-temperature sonicated for 30 min (5 °C, 40 kHz). The samples were chilled at − 20 °C for 30 min to precipitate the proteins. Subsequently, the samples were centrifuged for 15 min (4 °C, 13,000 g). The supernatant was carefully discarded, and the remaining residue was dried under a nitrogen stream. The dried sample was then re-dissolved in 100 µL of a solution consisting of acetonitrile and water in a 1:1 ratio. This reconstituted solution was further extracted through low-temperature ultrasonication for 5 min at 5 °C and 40 kHz. Finally, centrifugation was performed again at 13,000 g and 4 °C for 10 min, and the supernatant was carefully transferred into sample vials, ready for metabolomics analysis.

Liquid chromatography and mass spectrometry

Serum samples were separated and analyzed using the UHPLC-Q Exactive HF-X system (Thermo, USA). The ACQUITY UPLC BEH C18 column (1.7 µm, 3.0 × 100 mm, Waters, Milford, USA) was used as the chromatographic column. The column temperature was 40 ℃. Mobile phase A was water (containing 0.1% formic acid), and mobile phase B was acetonitrile/isopropanol (1/1) (containing 0.1% formic acid). At a flow rate of 0.4 mL/min and an injection volume of 2 µL, the elution gradient was processed in 10 min. By adjusting the ion spray voltage, the elution column was 0–3 min, 95–82% A; 3–9 min, 80–4% A; 9–13 min, 5–5% A; 13–13.1 min, 5–95% A; and 13.1–16 min, 95% A.

The collection of mass spectrometric data used the UHPLC-Q Exactive HF-X Mass Spectrometer (Thermo, USA), equipped with an electrospray ionization (ESI) source capable of operating in both positive and negative modes. Operating conditions were carefully calibrated, maintaining a sheath gas flow rate of 50 arb and an auxiliary gas flow rate of 13 arb. The source temperature was set to 425 °C. For positive mode, the ion spray voltage was precisely adjusted to 3500 V, whereas for negative mode, it was − 3500 V. The normalized collision energy follows a cyclic pattern of 20–40-60 V. The full mass spectrometry resolution was set at 60,000 for enhanced precision, while mass spectrometry/mass spectrometry resolution was set to 7500. Data acquisition was conducted in the data-dependent acquisition (DDA) mode, and the detection encompassed a mass range of 70–1050 m/z.

Method validation

During the quality control process, a pooled quality control sample (QC) was meticulously prepared by meticulously combining equal volumes of all samples. These QC samples were handled and assayed in an identical manner to the analytical

samples, ensuring their comparability. This approach effectively represented the entire sample set, facilitating regular monitoring of analysis stability through intermittent injection at fixed intervals (every 6 samples).

Data preprocessing and differential metabolite analysis

The raw data was imported into the Progression QI software for processing and metabolite identification. The metabolite information included the following: metabolite name, retention time, mass-to-charge ratio, and peak intensity. Internal standard peaks and false-positive peaks (including noise, column bleed, and derivatized reagent peaks) were removed from the data. The metabolites were identified by searching databases, and the main databases were the HMDB (http://www.hmdb.ca/) and Metlin (https://metlin.scripps.edu/). By the R package "ropls" (Version 1.6.2), the processed data were evaluated using principal component analysis (PCA) to assess the overall distribution of samples and the degree of dispersion between each group. The differential metabolites were screened by *T*-test and orthogonal partial least squares-discriminant analysis (OPLS-DA). Differential metabolite screening meets the conditions of VIP > 1 and $p < 0.05$. The reliability of the model fit was examined using a permutation test 200 times. The differential metabolites were enriched in the metabolic pathway through the KEGG database. Common pathways between transcriptomics and metabolomics were identified by Venn analysis using CTD software (Mo et al. 2022).

Western blot analysis

Protein expression of ABCG5, ABCG8, SULT2A1, OAT3, NCEH1, SLC10A1, KCNN2, GST, and NAT8 was analyzed by western blotting using the previously described method (Zhou et al. 2022).

Statistical analysis

The data were imported into GraphPad Prism 7.0 software for further analysis and generation of graphs, and the results were presented as mean ± SD. One-way ANOVA was used for statistical analysis to determine the significance of differences between multiple groups. A *p*-value of less than 0.05 was considered to indicate a statistically significant difference between the two groups.

Results

The effect of GE on ANIT-induced liver disease in rats

In this study, we evaluated the efficacy of GE in the treatment of IC through biochemical index and histological analyses. As demonstrated in Fig. 1a–f, a notable increase in the levels of ALT, AST, AKP, TBIL, DBIL, and TBA was observed in rats induced by ANIT compared to the control group. This elevation serves as a marker of liver injury, suggesting that the administration of ANIT caused harm to the hepatic tissue. Nevertheless, the administration of GE led to a substantial decrease in these biomarker levels, indicating a protective effect on the liver.

The histopathological examination further confirmed the biochemical findings. The hepatocytes of the control group rats exhibited an orderly arrangement with round nuclei and obvious nuclear membranes (Fig. 1g). In contrast, the ANIT group rats displayed a hazy and disorganized liver structure, along with increased liver cell volume, local necrosis, and inflammatory cell infiltration. Notably, the rats treated with GE exhibited a substantial reduction in these changes. The liver tissue stained with H&E from treatment groups exhibited a small amount of liver cell nucleus shrinkage and inflammatory cell infiltration. These findings highlight the significant inhibitory effect of GE on the formation of IC triggered by ANIT.

GE alleviated liver inflammation and oxidative stress in ANIT-induced rats

To investigate the ameliorative effects of GE on liver inflammation and oxidative stress in rats induced by ANIT, we assayed the concentrations of IL-β, IL-6, TNF-α, SOD, GSH, and MDA. In the ANIT-induced rats, significant elevations were observed in the levels of IL-β, IL-6, and TNF-α, along with marked reductions in SOD and GSH compared to the control group (Fig. 2a–f). These elevations were statistically significant ($p < 0.01$). GE treatment showed a dose-dependent improvement in these inflammatory and oxidative stress markers. In conclusion, our study demonstrates that GE may mitigate liver inflammation and oxidative stress in ANIT-induced rats.

Transcriptomic data analysis

To assess the molecular mechanism of GE in ANIT-induced rats, we extracted total RNAs from nine liver samples of the control, ANIT-induced, and GE high-dose groups. As shown in Fig. 3a, the expression of 2253 genes was significantly altered in the control group compared to the ANIT group, with 1283 genes up-regulated and 970 genes down-regulated. A total of 739 DEGs were screened to compare the differences between the ANIT group and the GE high-dose group, including 338 up-regulated genes and 401 down-regulated genes (Fig. 3b). These findings suggested that IC caused the activation of multiple pathways in the body.

To gain insights into the functions of these DEGs, we conducted a GO enrichment analysis. As shown in Fig. 3c

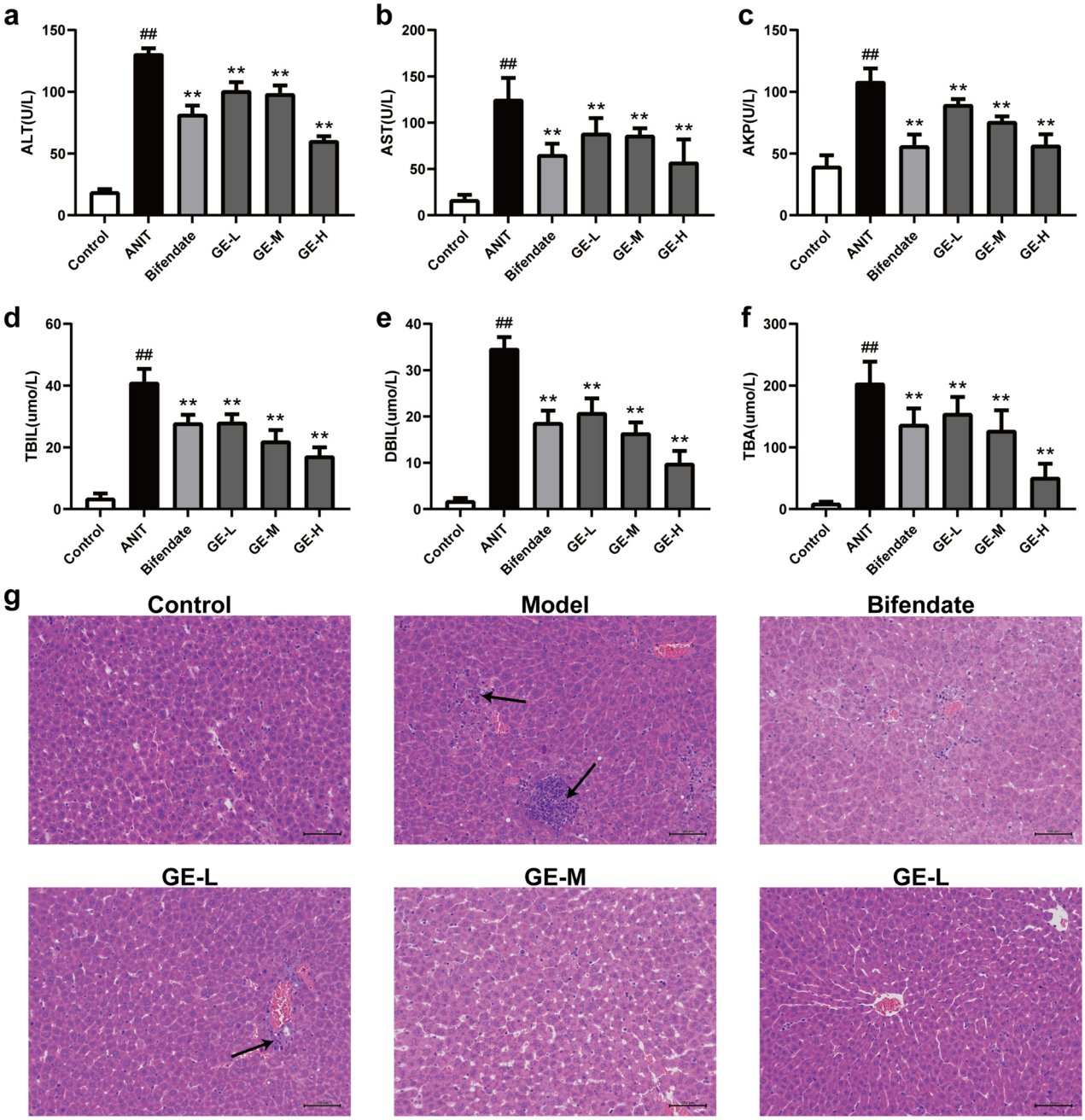

Fig. 1 Effects of GE on serum biochemical indexes and H&E staining (magnification: ×200) in rats with IC induced by ANIT. **a** Serum ALT level, **b** serum AST level, **c** serum AKP level, **d** serum TBIL level, **e** serum DBIL level, **f** serum TBA level, **g** H&E staining. Data are presented as mean ± SD ($n = 6$). #$p < 0.05$, ##$p < 0.01$ compared with the control group. *$p < 0.05$, **$p < 0.01$ compared with the ANIT group

and d, deregulated genes in the ANIT group, compared to the control group, were enriched in steroid biosynthesis, lipid oxidation, and neutrophil chemotaxis, targeting 35, 26, and 23 genes, respectively. In contrast, when comparing the GE group to the ANIT group, DEGs were primarily enriched in organic anion transport, steroid metabolic process, and cellular lipid catabolic process, with corresponding gene numbers of 35, 30, and 26. These processes are closely associated with cholestatic liver injury.

The KEGG pathway analysis showed 57 pathways in the control group versus the ANIT group (Fig. 3e). These pathways revealed their significance in various biological processes. Notably, the most prominent pathways were related to retinol metabolism, steroid hormone synthesis, linoleic

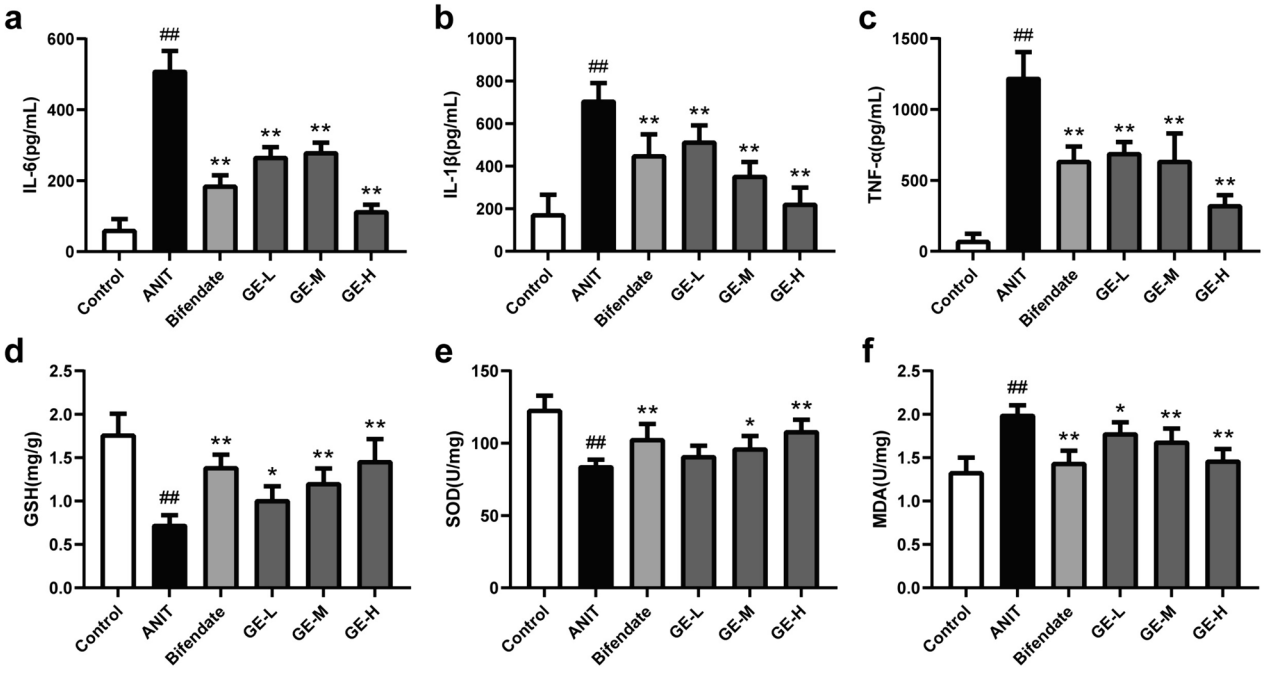

Fig. 2 Effects of GE on serum liver inflammation and oxidative stress levels in rats induced by ANIT. **a** IL-6 level, **b** IL-1β level, **c** TNF-α level, **d** content of GSH, **e** content of SOD, **f** content of MDA in different groups of rats ($n=6$). #$p<0.05$, ##$p<0.01$ compared with the control group. *$p<0.05$, **$p<0.01$ compared with the ANIT group

acid metabolism, PPAR signaling, and bile secretion. DEGs between the GE and ANIT groups revealed 30 significant pathways, mainly including retinol metabolism, steroid hormone synthesis, linoleic acid metabolism, PPAR signal transduction, arachidonic acid metabolism, and bile secretion, as shown in Fig. 3f. Among them, metabolic pathways were predominant, with a total of 18 pathways, followed by biological systems, with an enrichment of 16 pathways. Venn analysis identified 594 DEGs of the effect of GE on ANIT-induced IC. Figure 3h illustrates the KEGG pathway analysis of these DEGs.

Untargeted metabolomic data analysis

Multivariate statistical analysis

The control group, the GE high-dose group, and the ANIT group were selected to study the untargeted metabolomics. We evaluated the stability of the liquid chromatography and mass spectrometry/mass spectrometry (LC–MS/MS) model by analyzing score plots derived from the PCA and OPLS-DA models. The PCA score charts indicated that the LC–MS/MS method remained stable throughout the entire run, as evident from the high stability of QC in both positive and negative ionization modes (Fig. 4a and b). The OPLS-DA effectively separated the data among the three groups, revealing significant metabolomic differences between the control, GE high-dose, and ANIT groups (Fig. 4c–f). The model statistics R2X, R2Y, and Q2 in each group confirmed the reliability of the models and the absence of overfitting after 200 replacements (Fig. 4g and h).

Identification of metabolomic biomarkers

The metabolites fulfilling the criteria of $p<0.05$ in the *T*-test, VIP > 1, and multiple FC > 1 were chosen as differential metabolites. Comparing the GE group with the ANIT group, 98 differential metabolites were identified, with 41 metabolites being down-regulated and 57 metabolites being up-regulated. Furthermore, comparing the control group with the ANIT group, 158 differential biomarkers were screened out, of which 76 metabolites were up-regulated in serum and 82 metabolites were down-regulated. To investigate potential metabolic pathways, differential metabolites from both groups were imported into the scipy (Python) software for KEGG pathway enrichment analysis. This analysis resulted in the identification of 20 significant metabolic pathways based on their statistical significance ($p<0.01$).

As shown in Fig. 5b, the KEGG bubble chart demonstrates the primary impacts of ANIT on rats, including bile secretion, glutathione metabolism, ABC transporters, primary bile acid biosynthesis, aminoacyl-tRNA biosynthesis, and pantothenate and CoA biosynthesis metabolism. Figure 5b reveals that the effects of GE on IC in rats were

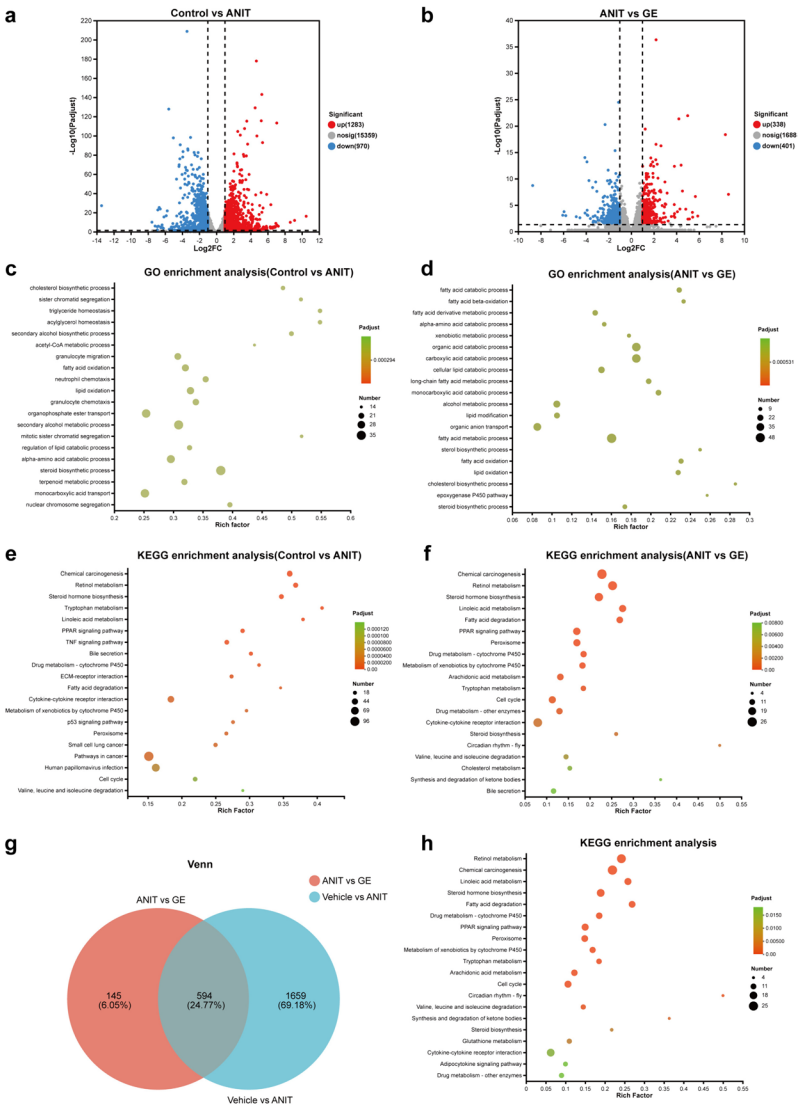

Fig. 3 Transcriptomic analysis of effects of GE in ANIT-induced rats. **a** Volcano diagram of the control group and the ANIT group. **b** Volcano diagram of the ANIT group and the GE group. **c** The GO terms of the control group and the ANIT group. **d** The GO terms of the ANIT group and the GE group. **e** The KEGG pathway analysis between the control group and the ANIT group. **f** The KEGG pathway analysis between the ANIT group and the GE group. **g** The Venn diagram of DEGs among groups. **h** The KEGG pathway analysis of 594 DEGs

associated with bile secretion, arginine and proline metabolism, beta-alanine metabolism, glutathione metabolism, primary bile acid biosynthesis, and glycerophospholipid metabolism signaling pathways. Comparing the ANIT-Control group with the GE-ANIT group, 42 metabolites were exclusively identified (Fig. 5c). Table 1 highlights the intersecting metabolites that could potentially serve as biomarker targets for GE's effect on IC. These 42 metabolites are enriched in 12 metabolic pathways, as depicted in Fig. 5d.

Integration analysis of transcriptomic and metabolomic data

Venn analysis was used to identify shared pathways enriched by transcriptomics and metabolomics datasets. We established a "genes-targets-pathways-compounds" network to elucidate the protective mechanism of GE against IC-type liver injury. The analysis revealed that bile secretion and glutathione metabolism were significantly enriched at the pathway level. Nine core targets were obtained, including ABCG5, ABCG8, SULT2A1, OAT3, NCEH1, SLC10A1, KCNN2, GST, and NAT8 (Fig. 6). Additionally, four differential metabolites were identified including glycocholic acid, spermidine, spermine, and taurocholic acid.

Protein expressions of GE on ANIT-induced rats

We evaluated the protein expression of the core targets by western blot analysis. The protein expression levels of NCEH1, OAT3, GST, and ABCG5 were notably down-regulated in the ANIT group compared to the control group. After intervention with GE, these protein expression levels significantly increased (Fig. 7). The protein expression levels of ABCG8, SULT2A1, SLC10A1, KCNN2, and NAT8 did not show statistically significant differences compared to the control group or after GE intervention.

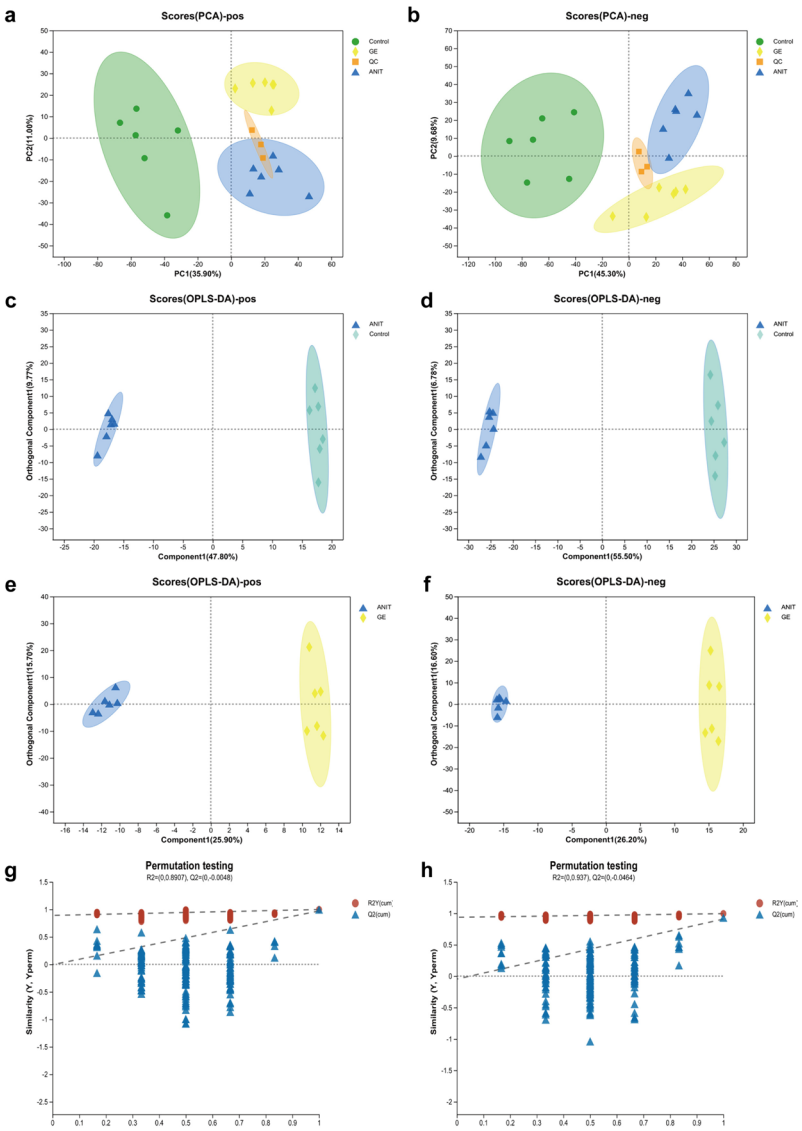

Fig. 4 Multivariate statistical analysis of metabolomics. **a**, **b** PCA score plots of positive and negative modes. **c**, **d** OPLS-DA score plots of control and ANIT in positive and negative modes. **e**, **f** OPLS-DA score plots of ANIT and GE in positive and negative modes. **g** 200-permutation test of the OPLS-DA model for the control group and the ANIT group. **h** 200-permutation test of the OPLS-DA model for the GE group and the ANIT group

Discussion

Transcriptomics primarily focuses on quantitatively assessing RNA transcripts of specific cells, tissues, or organs across diverse physiological and pathological conditions. The development of transcriptomics technology facilitates the investigation of the molecular basis of diseases and treatments (Hassan et al. 2020). However, a single-omics analysis method cannot fully understand the molecular regulatory network of complex biological systems (Yan et al. 2018). By integrating transcriptome and metabolome data at the pathway level, we can establish a correlation between differential genes and metabolites, enhancing our comprehension of drug treatment mechanisms (Lloyd-Price et al. 2019). In the present study, we used transcriptomics and metabolomics analysis for the first time to elucidate the therapeutic mechanism of GE in treating IC. We identified 739 genes regulated in the GE group compared to the ANIT group. The metabolomics results show that 98 differential metabolites were identified in the serum. Meanwhile, KEGG enrichment analysis revealed their main pathways. By jointly analyzing metabolomics and transcriptomics data, we identified two shared pathways as key regulators: bile secretion pathway and glutathione metabolism pathway. By further screening the proteins and biomarkers within these key pathways, we were able to pinpoint nine key proteins and four differential metabolites.

In this study, we established an ANIT model to assess the pharmacological effects of GE against IC. ANIT, a common cholestatic agent, has been extensively applied in numerous studies. Its administration causes metabolic disorders in liver tissue, leading to excessive accumulation of bile acids (Liu et al. 2022a, b; Shi et al. 2023). These characteristics are extremely similar to human acute cholestasis

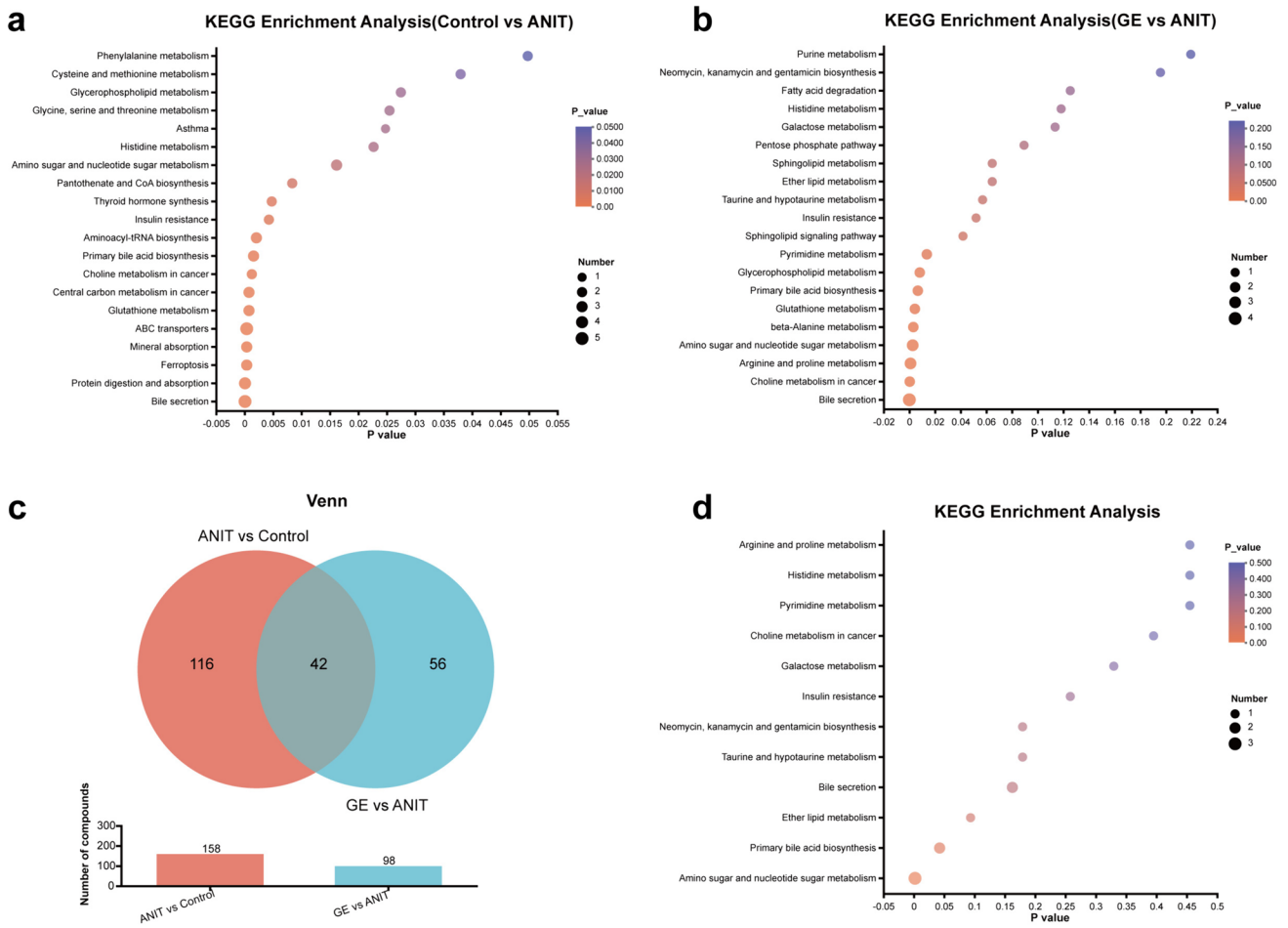

Fig. 5 Untargeted metabolomics analysis of effects of GE in ANIT-induced rats. **a** The KEGG pathway analysis of significantly differential metabolites between the ANIT group and the control group. **b** The KEGG pathway analysis of significantly differential metabolites between the ANIT group and the GE group. **c** Venn diagram of differential metabolites between the groups. **d** The KEGG pathway for 42 shared metabolites

liver injury (Tan et al. 2016a, b; Zhou et al. 2017). Cholestasis liver injury prompts the accumulation of harmful bile acids within the liver, subsequently triggering excessive ROS production and hepatic oxidative stress injury (Yi et al. 2018). This further causes a reduction of GSH and SOD levels within liver cells, an increase in MDA levels, and ultimately leads to liver cell death (Copple et al. 2010; Xiao et al. 2020). MDA, being a metabolic end product of lipid peroxides, can induce cytotoxicity by attacking polyunsaturated fatty acids present in cell membranes (Lixin et al. 2019). On the other hand, SOD functions as the primary anti-oxidative enzyme, catalyzing the dismutation of free radicals to produce oxygen and hydrogen peroxide, thereby mitigating cell damage (Wu et al. 2017a, b). GSH acts as a powerful scavenger, safeguarding the liver from oxidative stress and detoxifying various electrophilic compounds and peroxides (Wang et al. 2017). Hence, MDA, SOD, and GSH are often considered as reliable markers of oxidative stress. In addition, the excessive oxidative stress response triggered by cholestasis can activate the inflammatory signaling pathway, leading to an increase in serum inflammatory factor levels and accelerating the development of liver injury (Gao et al. 2024). Bifendate is widely used in clinical settings as a hepatoprotective agent, especially in the treatment of drug-induced liver injury (Pan et al. 2006). In rats models, bifendate serves as a frequently employed positive control for the investigation of liver-protective agents (Talifu et al. 2019). Compared to OCA and UDCA, bifendate exhibits a significant and rapid effect in reducing serum ALT, AST, and AKP levels in patients experiencing drug-induced elevations, while its adverse reactions tend to be relatively minor. In this study, GE significantly reduced the serum levels of ALT, AST, AKP, TBIL, DBIL, and TBA in ANIT-induced IC rats. Additionally, GE reversed the inflammatory response and oxidative stress induced by ANIT, suppressing the expression of inflammatory factors (TNF-α, IL-6, and

Table 1 Differential metabolite information in serum

Metabolite	Formula	Mode	M/Z	Retention time	*p*-value		Regulate	
					ANIT/GE	Control/ANIT	ANIT/GE	Control/ANIT
UDP-D-galactose	C15H24N2O17P2	Neg	565.047733	0.714116667	0.01159	1.98E − 06	Down	Down
Taurocholic acid	C26H45NO7S	Neg	514.2833362	3.841333333	0.01648	2.91E − 06	Up	Down
Taurochenodeoxycholate-3-sulfate	C26H45NO9S2	Neg	288.6194878	4.503	0.0102	9.67E − 10	Up	Down
Uridine diphosphate-N-acetylglucosamine	C17H27N3O17P2	Neg	606.074702	0.714116667	0.0252	4.71E − 06	Down	Down
Endalin	C9H12FN3O3	Neg	264.0547374	1.023066667	0.00789	2.05E − 05	Up	Down
Ferulic acid 4-sulfate	C10H10O7S	Neg	273.0075608	1.666483333	0.0315	9.74E − 05	Up	Down
N-Palmitoyl phenylalanine	C25H41NO3	Neg	448.3069764	5.0771	0.007149	2.26E − 06	Down	Up
Lithocholic acid glycine conjugate	C26H43NO4	Neg	478.3170339	5.249466667	0.004699	0.004178	Down	Up
Deoxycholic acid glycine conjugate	C26H43NO5	Neg	448.30678	6.148933333	0.003574	4.18E − 07	Down	Up
N-palmitoyl taurine	C18H37NO4S	Neg	362.2368386	7.64115	0.006509	0.004639	Up	Down
N-arachidonoyl taurine	C22H37NO4S	Neg	410.2369581	7.2037	0.003283	0.009952	Up	Down
(S)-Nerolidol 3-O-[a-L-rhamnopyranosyl-(1- > 2)-b-D-glucopyranoside]	C27H46O10	Neg	565.2836405	4.769133333	0.02228	1.32E − 05	Up	Down
Ceanothine E	C34H40N4O4	Neg	567.2996403	4.331866667	0.002155	4.91E − 06	Up	Down
4-Hydroxy-17beta-estradiol-2-S-glutathione	C28H39N3O9S	Neg	614.2095787	3.841333333	0.01514	2.98E − 06	Up	Down
4-Hydroxy-5-(3′,4′-dihydroxyphenyl)-valeric acid-O-methyl-O-glucuronide	C18H26O12	Neg	433.1351519	1.94565	9.90E-09	0.007888	Down	Up
4-Vinylphenol sulfate	C8H8O4S	Neg	245.0121832	1.78845	0.01535	0.0004481	Up	Down
[(3-Phenyloxiran-2-yl)methoxy]sulfonic acid	C9H10O5S	Neg	275.0232641	1.64905	0.004871	5.54E − 05	Up	Down
Imidazoleacetic acid ribotide	C10H15N2O9P	Neg	337.0442939	0.820183333	0.01284	4.56E − 06	Down	Down
Cytidine	C9H13N3O5	Neg	242.0793118	0.597266667	0.01631	3.73E − 07	Down	Up
N-Methyl-1-deoxynojirimycin	C7H15NO4	Neg	214.0479729	0.597266667	0.001877	9.78E − 08	Down	Up
Glycocholic acid	C26H43NO6	Pos	430.2938725	4.145033333	0.02748	0.01529	Down	Up
4-Guanidinobutanoic acid	C5H11N3O2	Pos	146.091849	0.6514	0.02612	2.10E − 05	Up	Down
Ribothymidine	C10H14N2O6	Pos	259.0914925	0.637416667	0.001951	0.0001755	Up	Down
Gravacridonediol	C19H19NO5	Pos	364.1160821	1.302783333	0.0466	1.02E − 07	Up	Down
Delta-valerolactam	C5H9NO	Pos	100.0757667	1.3181	0.006456	0.0004862	Up	Down
N-Deschlorobenzoyl indomethacin	C12H13NO3	Pos	202.085614	1.85045	0.04305	1.12E − 08	Up	Down
1-Methyl-3-(2-thiazolyl)-1H-indole	C12H10N2S	Pos	247.0890629	3.275	0.02306	0.001901	Up	Down
(1xi,3xi)-1,2,3,4-Tetrahydro-1-methyl-beta-carboline-3-carboxylic acid	C13H14N2O2	Pos	231.1119795	3.306116667	0.01065	5.81E − 09	Up	Down
Tauroursodeoxycholic acid	C26H45NO6S	Pos	464.2814748	4.710016667	0.0005007	0.003924	Down	Up
7Z,10Z-Hexadecadienoic acid	C16H28O2	Pos	543.3812	9.12625	0.001403	0.01215	Down	Down
PC(19:0/0:0)	C27H56NO7P	Pos	538.3851431	9.065683333	0.007858	1.85E − 05	Down	Up
13-HDoHE	C22H34O	Pos	337.2513189	5.227366667	0.001749	0.004545	Down	Up
N-Oleoyl GABA	C22H41NO3	Pos	412.2832654	5.227366667	0.002852	0.001407	Down	Up

Table 1 (continued)

Metabolite	Formula	Mode	M/Z	Retention time	*p*-value		Regulate	
					ANIT/GE	Control/ANIT	ANIT/GE	Control/ANIT
Ginsenoside Rd	C48H82O18	Pos	979.5880949	4.556333333	0.008818	0.01337	Down	Down
1-(4-Hydroxyphenyl)-1-decene-3,5-dione	C16H20O3	Pos	261.1476088	4.540933333	0.02113	1.19E − 09	Down	Up
Polyporusterone B	C28H44O6	Pos	540.3338042	3.83145	0.008964	9.35E − 08	Up	Down
Phenylalanyl-lysine	C15H23N3O3	Pos	316.1644835	2.890833333	0.0002455	9.03E − 05	Up	Down
3-Hydroxy-2-methylglutarate	C7H12O5	Pos	141.0541432	1.669766667	0.0002149	3.45E − 08	Up	Down
N-Monodesmethyl-rizatriptan	C15H19N5O	Pos	318.1900137	1.381083333	0.002476	0.0001396	Up	Down
Glycyl-lysine	C8H17N3O3	Pos	245.1598406	0.88095	0.001385	6.20E − 10	Up	Down
Isoputreanine	C7H16N2O2	Pos	193.1540638	0.623433333	0.004452	0.001295	Up	Down
Glycerophosphocholine	C8H20NO6P	Pos	296.0649957	0.58115	0.03036	1.88E − 05	Down	Up

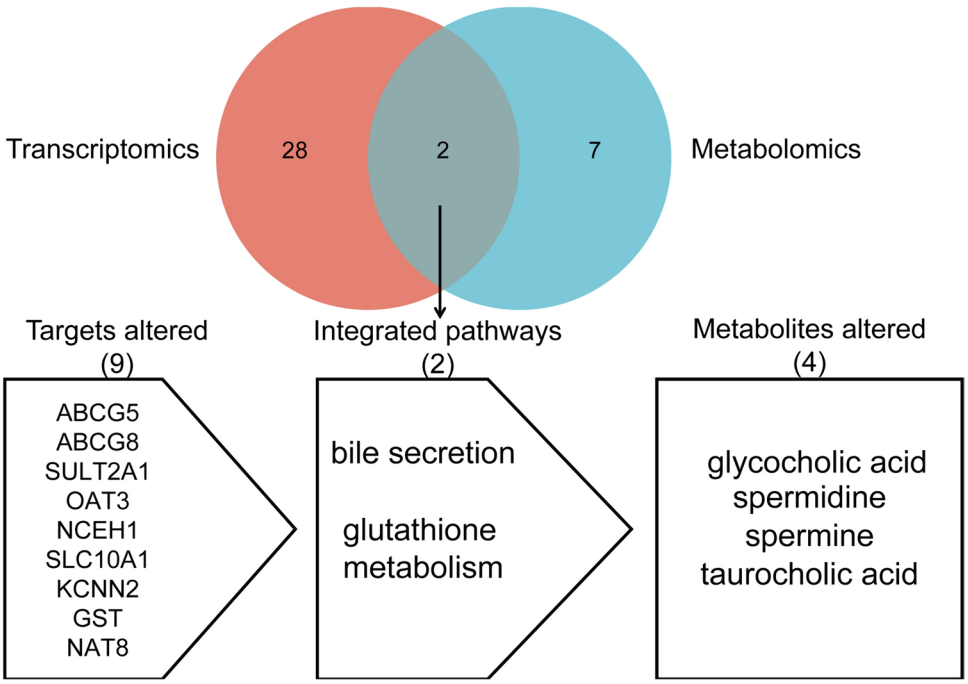

Fig. 6 Venn diagram of the transcriptomic and metabolomic enriched pathway

IL-1β), reducing MDA content, and increasing the activity of SOD and GHS. In conclusion, these results illustrated that GE could repair the liver injury by mitigating the level of oxidative stress and reducing inflammatory response.

To gain a deeper understanding of the regulation of potential biomarkers in the GE group, we devised a novel approach employing the "genes-targets-pathways-compounds" network for analyzing the potential targets and biomarkers GE against ANIT-induced IC. By the integration of metabolomics and transcriptomics data, we pinpointed 2 shared pathways: the bile secretion pathway and the glutathione pathway. Within these key pathways, we screened and identified a total of nine critical targets and four metabolites. We validated these targets through western blotting. The findings demonstrated a notable increase in the expression levels of ABCG5, NCEH1, GST, and OAT3 proteins following GE intervention. We speculate that the mechanism of GE against ANIT-induced IC is related to these proteins.

Bile acids play a crucial role in the efflux and metabolism of cholesterol, toxic exogenous, and endogenous substances (Boyer 2013). As the end products of cholesterol catabolism, bile acids are essential for maintaining cholesterol homeostasis and preventing lipid accumulation in the liver and other organs (Chiang 2013). In the gallbladder, cholesterol is secreted into the bile, combining with

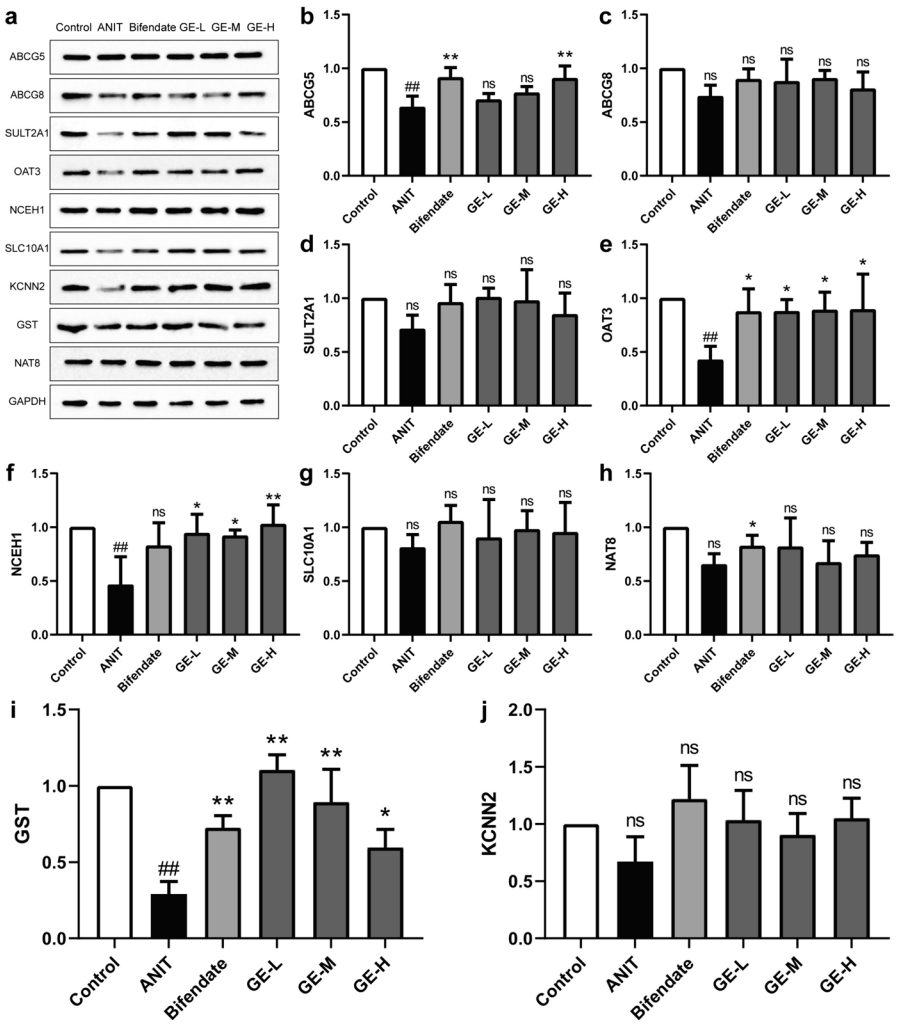

Fig. 7 Expression levels of different proteins in the liver tissue. **a** Electrophoretic diagram of different groups. **b–j** Expressions of ABCGG, ABCG8, SULT2A1, OAT3, NECH1, SLC10A1, NAT8, GST, and KCNN2 protein ($n=3$). ##$p<0.01$, ###$p<0.001$ compared with control group. *$p<0.05$, **$p<0.01$ compared with ANIT group. Ns represents no significant difference

phospholipids and bile acids to form mixed micelles. This process prevents the precipitation of cholesterol in the gallbladder, thereby mitigating the potential for further liver damage caused by cholesterol accumulation (Small 2003). The excretion of cholesterol in bile is primarily mediated by the heteromeric transporters ABCG5/8 (Graf et al. 2003). These transmembrane proteins are primarily expressed in liver cells and regulate the directed transport of cholesterol from the liver to bile. An imbalance in ABCG5 and ABCG8 can lead to obstruction of cholesterol metabolism and bile secretion, ultimately exacerbating liver disease development (Zein et al. 2019). A study focusing on the mechanism of ABCG5/8 in cholesterol secretion found that mice lacking the ABCG5/8 heterodimer exhibited a notable inhibition in cholesterol excretion into bile (Yu et al. 2002). Conversely, mice overexpressing ABCG5/8 exhibited enhanced biliary cholesterol secretion and reduced absorption of dietary sterols. Consistent with our findings, the expression level of ABCG5 was significantly reduced in the ANIT-induced IC rats. Intervention with GE in rats significantly increased the expression of ABCG5, indicating that GE enhances cholesterol transport capacity and reduces liver damage caused by cholestasis. The previous study demonstrated that the occurrence of cholestasis is highly correlated with hypercholesterolemia (Wang et al. 2015). When bile flow decreases or becomes blocked, cholesterol accumulates in hepatic cells, leading to cholesterolemia (Kowdley et al. 2018). NCEH1, also known as AADACL1, promotes the metabolism of cholesterol by catalyzing the hydrolysis of cholesterol esters into fatty acids and free cholesterol, thereby reducing the occurrence of cholesterolemia caused by cholestasis (Zhao et al. 2008). Previous research demonstrated that overexpressing NCEH1 in rats had significantly increased bile acid secretion into the bile and elevated cholesterol levels in gallbladder bile and feces (Wang et al. 2015). This finding indicated that the expression of NCIH1 in the liver had a significant impact on the secretion of bile acids and the clearance of cholesterol. In our study, GE intervention increased the expression of NCEH1, suggesting that GE could potentially enhance the catabolism of cholesterol and

alleviate the symptoms of cholesterolemia. In terms of bile metabolism, the SLC22 transporter family plays a crucial role in the uptake and efflux of bile acids (Nigam 2018). Among its members, OAT3 is responsible for the transport of endogenous compounds such as bile acids (Johnston et al. 2014). Our study demonstrated that the expression of OAT3 was significantly increased after high-dose GE intervention, indicating that GE may alleviate cholestasis by regulating bile acid excretion.

It is widely acknowledged that excessive oxidation occurs during ANIT-induced liver injury (Wu et al. 2017a, b). GSH serves as a crucial antioxidant and redox regulator within cells, playing a vital role in counteracting the oxidation of cellular components (Lu 2009). It is particularly effective in neutralizing free radicals and enhancing oxidative stress defense mechanisms. Notably, GSH concentrations are highest in the liver and kidney. Under physiological conditions, the liver is protected from oxidative stress by synthesizing GSH (Garcia-Ruiz and Fernandez-Checa 2006). Numerous studies conducted on humans and animals have highlighted the significance of disrupted GSH homeostasis in the development of hepatopathies. In the context of cholestatic liver injury, chronic exposure to toxic bile acids can cause oxidative stress, apoptosis, and fibrosis, ultimately leading to cirrhosis (Chen et al. 2013). The GSH protective mechanism against liver injury is facilitated by the catalytic action of GST (Nigam 2018). This enzyme catalyzes the binding of GSH to various endogenous and exogenous electrophilic molecules (Kumar et al. 2017). This conjugation reaction aids in detoxifying and eliminating harmful oxidants, thereby mitigating the damaging effects of oxidative stress. In our study, the protective mechanism of GE against ANIT-induced liver injury primarily focuses on the glutathione metabolic pathway. Specifically, we observed an increase in GST expression following GE intervention. GE may alleviate the oxidative stress response in hepatocytes by catalyzing the binding of GSH to toxic ANIT.

Conclusions

In this study, we utilized an integration of metabolomics and transcriptomics for the first time to elucidate the mechanisms of GE in treating IC rats. The results indicated that GE exhibits a protective effect against IC-type injury. We speculated that the potential mechanism of GE was related to regulating the bile secretion pathway and glutathione pathway. However, it remains unclear whether GE directly interacts with these targets, necessitating further pharmacological experiments to elucidate the precise mechanisms. Our study provided a theoretical basis for the development of new drugs and the treatment of cholestasis.

Author contribution Conceptualization, G.L.; methodology, Y.C.; software, Y.C.; investigation, J.Z.; data curation, J.Z.; writing—original draft preparation, J.Z.; writing—review and editing, G.L. and Y.L.; visualization, Y.C. and Y.L.; supervision, G.L.; project administration, G.L. All authors have read and agreed to the published version of the manuscript. The authors declare that all data were generated in-house and that no paper mill was used.

Funding This research was supported by the National Key Basic Research and Development Program in China (2017YFC1700902), the Research on the Protective Mechanism of Saffron I on ANIT Induced Liver Injury Project (202311148), the Physiological Response and Molecular Mechanism of Iron Deficiency Yellowing in *Gardenia jasminoides* Ellis (2022B1043), and the Study on the Seed and Seedling Standards of Excellent Gardenia Seed Line.

Data availability The RNA-seq data can be found in NCBI, under the accession number of PRJNA934684.

Declarations

Ethical approval All experimental procedures were approved by the Animal Ethics Committee of the Jiangxi University of Chinese Medicine (Approval No.: JZLLSC20220579).

Conflict of interest The authors declare no competing interests.

References

Boyer JL (2013) Bile Formation and Secretion. Compr Physiol 3(3):1035–1078. https://doi.org/10.1002/cphy.c120027

Chen Y, Dong H, Thompson DC, Shertzer HG, Nebert DW, Vasiliou V (2013) Glutathione defense mechanism in liver injury: insights from animal models. Food Chem Toxicol 60:38–44. https://doi.org/10.1016/j.fct.2013.07.008

Chiang JY (2013) Bile acid metabolism and signaling. Compr Physiol 3(3):1191–1212. https://doi.org/10.1002/cphy.c120023

Copple BL, Jaeschke H, Klaassen CD (2010) Oxidative stress and the pathogenesis of cholestasis. Semin Liver Dis 30(2):195–204. https://doi.org/10.1055/s-0030-1253228

Corpechot C, Chazouillères O, Poupon R (2011) Early primary biliary cirrhosis: biochemical response to treatment and prediction of long-term outcome. J Hepatol 55(6):1361–1367. https://doi.org/10.1016/j.jhep.2011.02.031

Fang S, Wang T, Li Y, Xue H, Zou J, Cai J et al (2022) Gardenia jasminoides Ellis polysaccharide ameliorates cholestatic liver injury by alleviating gut microbiota dysbiosis and inhibiting the TLR4/NF-κB signaling pathway. Int J Biol Macromol 205:23–36. https://doi.org/10.1016/j.ijbiomac.2022.02.056

Gao S, Feng Q (2022) The beneficial effects of geniposide on glucose and lipid metabolism: a review. Drug Des Devel Ther 16:3365–3383. https://doi.org/10.2147/DDDT.S378976

Gao Q, Li G, Zu Y, Xu Y, Wang C, Xiang D et al (2024) Ginsenoside Rg1 alleviates ANIT-induced cholestatic liver injury by inhibiting hepatic inflammation and oxidative stress via SIRT1 activation. J Ethnopharmacol 319(Pt 1):117089. https://doi.org/10.1016/j.jep.2023.117089

Garcia-Ruiz C, Fernandez-Checa JC (2006) Mitochondrial glutathione: hepatocellular survival-death switch. J Gastroenterol Hepatol 21(Suppl 3):S3–S6. https://doi.org/10.1111/j.1440-1746.2006.04570.x

Graf GA, Yu L, Li WP, Gerard R, Tuma PL, Cohen JC et al (2003) ABCG5 and ABCG8 are obligate heterodimers for

protein trafficking and biliary cholesterol excretion. J Biol Chem 278(48):48275–48282. https://doi.org/10.1074/jbc.M310223200
Hassan S, Hertel P (2022) Overview of progressive familial intrahepatic cholestasis. Clin Liver Dis 26(3):371–390. https://doi.org/10.1016/j.cld.2022.03.003
Hassan MA, Al-Sakkaf K, Shait Mohammed MR, Dallol A, Al-Maghrabi J, Aldahlawi A et al (2020) Integration of transcriptome and metabolome provides unique insights to pathways associated with obese breast cancer patients. Front Oncol 10:804. https://doi.org/10.3389/fonc.2020.00804
Hirschfield GM, Mason A, Luketic V, Lindor K, Gordon SC, Mayo M et al (2015) Efficacy of obeticholic acid in patients with primary biliary cirrhosis and inadequate response to ursodeoxycholic acid. Gastroenterology 148(4):751–61.e8. https://doi.org/10.1053/j.gastro.2014.12.005
Hobson S, Gandhi S, Sobel M (2022) Intrahepatic cholestasis of pregnancy. CMAJ 194(48):E1650. https://doi.org/10.1503/cmaj.220334
Hu L, Zhao J, Liu Y, Liu X, Lu Q, Zeng Z et al (2020) Geniposide inhibits proliferation and induces apoptosis of diffuse large B-cell lymphoma cells by inactivating the HCP5/miR-27b-3p/MET axis. Int J Med Sci 17(17):2735–2743. https://doi.org/10.7150/ijms.51329
Ivashkin VT, Maevskaya MV, Kobalava ZD, Uspenskiy YP, Fominih JA, Rozanov AV et al (2018) Open-label study of ademetionine for the treatment of intrahepatic cholestasis associated with alcoholic liver disease. Minerva Gastroenterol Dietol 64(3):208–219. https://doi.org/10.23736/S1121-421X.18.02461-3
Jin Z, Chang B, Wei Y, Yang Y, Zhang H, Liu J et al (2022) Curcumin exerts chondroprotective effects against osteoarthritis by promoting AMPK/PINK1/Parkin-mediated mitophagy. Biomed Pharmacother 151:113092. https://doi.org/10.1016/j.biopha.2022.113092
Johnston RA, Rawling T, Chan T, Zhou F, Murray M (2014) Selective inhibition of human solute carrier transporters by multikinase inhibitors. Drug Metab Dispos 42(11):1851–1857. https://doi.org/10.1124/dmd.114.059097
Kim HY (2021) Recent advances in nonalcoholic fatty liver disease metabolomics. Clin Mol Hepatol 27(4):553–559. https://doi.org/10.3350/cmh.2021.0127
Kowdley KV, Luketic V, Chapman R, Hirschfield GM, Poupon R, Schramm C et al (2018) A randomized trial of obeticholic acid monotherapy in patients with primary biliary cholangitis. Hepatology 67(5):1890–1902. https://doi.org/10.1002/hep.29569
Kumar A, Dhull DK, Gupta V, Channana P, Singh A, Bhardwaj M et al (2017) Role of glutathione-S-transferases in neurological problems. Expert Opin Ther Pat 27(3):299–309. https://doi.org/10.1080/13543776.2017.1254192
Levy C, Manns M, Hirschfield G (2023) New treatment paradigms in primary biliary cholangitis. Clin Gastroenterol Hepatol 21(8):2076–2087. https://doi.org/10.1016/j.cgh.2023.02.005
Liu J, Liu J, Meng C, Huang C, Liu F, Xia C (2022a) Oleanolic acid alleviates ANIT-induced cholestatic liver injury by activating Fxr and Nrf2 pathways to ameliorate disordered bile acids homeostasis. Phytomedicine 102:154173. https://doi.org/10.1016/j.phymed.2022.154173
Liu J, Song C, Nie C, Sun Y, Wang Y, Xue L et al (2022b) A novel regulatory mechanism of geniposide for improving glucose homeostasis mediated by circulating RBP4. Phytomedicine 95:153862. https://doi.org/10.1016/j.phymed.2021.153862
Lixin X, Erli G, Songping H, Yonggen Z, Wang J, Lijun Y (2019) Yi Guan Jian, A traditional chinese herbal medicine, alleviates carbon tetrachloride-induced liver injury. Evid Based Complement Alternat Med 2019:9824728. https://doi.org/10.1155/2019/9824728
Lloyd-Price J, Arze C, Ananthakrishnan AN, Schirmer M, Avila-Pacheco J, Poon TW et al (2019) Multi-omics of the gut microbial ecosystem in inflammatory bowel diseases. Nature 569(7758):655–662. https://doi.org/10.1038/s41586-019-1237-9
Lu SC (2009) Regulation of glutathione synthesis. Mol Aspects Med 30(1–2):42–59. https://doi.org/10.1016/j.mam.2008.05.005
Menyhárt O, Győrffy B (2021) Multi-omics approaches in cancer research with applications in tumor subtyping, prognosis, and diagnosis. Comput Struct Biotechnol J 19:949–960. https://doi.org/10.1016/j.csbj.2021.01.009
Misra BB, Langefeld CD, Olivier M, Cox LA (2018) Integrated omics: tools, advances, and future approaches. J Mol Endocrinol 18–0055. https://doi.org/10.1530/JME-18-0055
Mo L, Ma C, Wang Z, Li J, He W, Niu W et al (2022) Integrated bioinformatic analysis of the shared molecular mechanisms between osteoporosis and atherosclerosis. Front Endocrinol (lausanne) 13:950030. https://doi.org/10.3389/fendo.2022.950030
Nigam SK (2018) The SLC22 transporter family: a paradigm for the impact of drug transporters on metabolic pathways, signaling, and disease. Annu Rev Pharmacol Toxicol 58:663–687. https://doi.org/10.1146/annurev-pharmtox-010617-052713
Pan SY, Yang R, Han YF, Dong H, Feng XD, Li N et al (2006) High doses of bifendate elevate serum and hepatic triglyceride levels in rabbits and mice: animal models of acute hypertriglyceridemia. Acta Pharmacol Sin 27(6):673–678. https://doi.org/10.1111/j.1745-7254.2006.00332.x
Pfister ED, Dröge C, Liebe R, Stalke A, Buhl N, Ballauff A et al (2022) Extrahepatic manifestations of progressive familial intrahepatic cholestasis syndromes: presentation of a case series and literature review. Liver Int 42(5):1084–1096. https://doi.org/10.1111/liv.15200
Picard M, Scott-Boyer MP, Bodein A, Périn O, Droit A (2021) Integration strategies of multi-omics data for machine learning analysis. Comput Struct Biotechnol J 19:3735–3746. https://doi.org/10.1016/j.csbj.2021.06.030
Salmen F, De Jonghe J, Kaminski TS, Alemany A, Parada GE, Verity-Legg J et al (2022) High-throughput total RNA sequencing in single cells using VASA-seq. Nat Biotechnol 40(12):1780–1793. https://doi.org/10.1038/s41587-022-01361-8
Santos AA, Delgado TC, Marques V, Ramirez-Moncayo C, Alonso C, Vidal-Puig A et al (2023) Spatial metabolomics and its application in the liver. Hepatology 79(5):1158–1179. https://doi.org/10.1097/HEP.0000000000000341
Saviano A, Henderson NC, Baumert TF (2020) Single-cell genomics and spatial transcriptomics: discovery of novel cell states and cellular interactions in liver physiology and disease biology. J Hepatol 73(5):1219–1230. https://doi.org/10.1016/j.jhep.2020.06.004
Shi L, Zhao T, Huang L, Pan X, Wu T, Feng X et al (2023) Engineered FGF19ΔKLB protects against intrahepatic cholestatic liver injury in ANIT-induced and Mdr2-/- mice model. BMC Biotechnol 23(1):43. https://doi.org/10.1186/s12896-023-00810-9
Small DM (2003) Role of ABC transporters in secretion of cholesterol from liver into bile. Proc Natl Acad Sci USA 100(1):4–6. https://doi.org/10.1073/pnas.0237205100
Song D, Zhu P, Dong Y, Wang M, Zhao A, Xia H et al (2023) Mechanism of crocin I on ANIT-induced intrahepatic cholestasis by combined metabolomics and transcriptomics. Front Pharmacol 13:1088750. https://doi.org/10.3389/fphar.2022.1088750
Talifu A, Saimaiti R, Maitinuer Y, Liu G, Abudureyimu M, Xin X (2019) Multiomics analysis profile acute liver injury module clusters to compare the therapeutic efficacy of bifendate and muaddil sapra. Sci Rep 9(1):4335. https://doi.org/10.1038/s41598-019-40356-5
Tan Z, Liu A, Luo M, Yin X, Song D, Dai M et al (2016a) Geniposide inhibits alpha-naphthylisothiocyanate-induced intrahepatic cholestasis: the downregulation of STAT3 and NFkB signaling plays an important role. Am J Chin Med 44(4):721–736. https://doi.org/10.1142/S0192415X16500397

Tan Z, Luo M, Yang J, Cheng Y, Huang J, Lu C et al (2016b) Chlorogenic acid inhibits cholestatic liver injury induced by α-naphthylisothiocyanate: involvement of STAT3 and NFκB signalling regulation. J Pharm Pharmacol 68(9):1203–1213. https://doi.org/10.1111/jphp.12592

van Hooff MC, Werner E, van der Meer AJ (2024) Treatment in primary biliary cholangitis: beyond ursodeoxycholic acid. Eur J Intern Med 124:14–21. https://doi.org/10.1016/j.ejim.2024.01.030

Vitale G, Mattiaccio A, Conti A, Berardi S, Vero V, Turco L et al (2023) Molecular and clinical links between drug-induced cholestasis and familial intrahepatic cholestasis. Int J Mol Sci 24(6):5823. https://doi.org/10.3390/ijms24065823

Wang JM, Wang D, Tan YY, Zhao G, Ji ZL (2015) Pioglitazone reduces lipid droplets in cholesterolosis of the gallbladder by increasing ABCA1 and NCEH1 expression. Mol Cell Biochem 399(1–2):7–15. https://doi.org/10.1007/s11010-014-2225-x

Wang MY, Srinivasan M, Dasari S, Narvekar P, Samy ALPA, Dontaraju VS et al (2017) Antioxidant activity of Yichun blue honeysuckle (YBHS) berry counteracts CCl_4-induced toxicity in liver injury model of mice. Antioxidants (basel) 6(3):50. https://doi.org/10.3390/antiox6030050

Wu JS, Li YF, Li YY, Dai Y, Li WK, Zheng M et al (2017a) Huangqi decoction alleviates alpha-naphthylisothiocyanate induced intrahepatic cholestasis by reversing disordered bile acid and glutathione homeostasis in mice. Front Pharmacol 8:938. https://doi.org/10.3389/fphar.2017.00938

Wu T, Li J, Li Y, Song H (2017b) Antioxidant and hepatoprotective effect of swertiamarin on carbon tetrachloride-induced hepatotoxicity via the Nrf2/HO-1 pathway. Cell Physiol Biochem 41(6):2242–2254. https://doi.org/10.1159/000475639

Xiao Q, Zhang S, Ren H, Du R, Li J, Zhao J et al (2020) Ginsenoside Rg1 alleviates ANIT-induced intrahepatic cholestasis in rats via activating farnesoid X receptor and regulating transporters and metabolic enzymes. Chem Biol Interact 324:109062. https://doi.org/10.1016/j.cbi.2020.109062

Yan J, Risacher SL, Shen L, Saykin AJ (2018) Network approaches to systems biology analysis of complex disease: integrative methods for multi-omics data. Brief Bioinform 19(6):1370–1381. https://doi.org/10.1093/bib/bbx066

Yi YX, Ding Y, Zhang Y, Ma NH, Shi F, Kang P et al (2018) Yinchenhao decoction ameliorates alpha-naphthylisothiocyanate induced intrahepatic cholestasis in rats by regulating phase II metabolic enzymes and transporters. Front Pharmacol 9:510. https://doi.org/10.3389/fphar.2018.00510

Yu L, Hammer RE, Li-Hawkins J, Von Bergmann K, Lutjohann D, Cohen JC et al (2002) Disruption of Abcg5 and Abcg8 in mice reveals their crucial role in biliary cholesterol secretion. Proc Natl Acad Sci USA 99(25):16237–16242. https://doi.org/10.1073/pnas.252582399

Yuan J, Zhang J, Cao J, Wang G, Bai H (2020) Geniposide alleviates traumatic brain injury in rats via anti-inflammatory effect and MAPK/NF-kB inhibition. Cell Mol Neurobiol 40(4):511–520. https://doi.org/10.1007/s10571-019-00749-6

Zein AA, Kaur R, Hussein TOK, Graf GA, Lee JY (2019) ABCG5/G8: a structural view to pathophysiology of the hepatobiliary cholesterol secretion. Biochem Soc Trans 47(5):1259–1268. https://doi.org/10.1042/BST20190130

Zhao B, Song J, Ghosh S (2008) Hepatic overexpression of cholesteryl ester hydrolase enhances cholesterol elimination and in vivo reverse cholesterol transport. J Lipid Res 49(10):2212–2217. https://doi.org/10.1194/jlr.M800277-JLR200

Zhou HQ, Liu W, Wang J, Huang YQ, Li PY, Zhu Y et al (2017) Paeoniflorin attenuates ANIT-induced cholestasis by inhibiting apoptosis in vivo via mitochondria-dependent pathway. Biomed Pharmacother 89:696–704. https://doi.org/10.1016/j.biopha.2017.02.084

Zhou Y, Zhou Y, Li Y, Sun W, Wang Z, Chen L et al (2022) Targeted bile acid profiles reveal the liver injury amelioration of Da-Chai-Hu decoction against ANIT- and BDL-induced cholestasis. Front Pharmacol 13:959074. https://doi.org/10.3389/fphar.2022.959074

Zhou YX, Zhang RQ, Rahman K, Cao ZX, Zhang H, Peng C (2019) Diverse pharmacological activities and potential medicinal benefits of geniposide. Evid Based Complement Alternat Med 4925682. https://doi.org/10.1155/2019/4925682